Optics and Lasers in Engineering 50 (2012) 540–546

Contents lists available at ScienceDirect

Optics and Lasers in Engineering

journal homepage: www.elsevier.com/locate/optlaseng

The mass transfer process and the growth rate of NaCl crystal growth by evaporation based on temporal phase evaluation

Zhao Jing[a], Miao Hong[a,*], Duan Li[b], Kang Qi[b], He Linghui[a]

[a] Key Laboratory of Mechanical Behavior and Design of Materials (CAS), Department of Modern Mechanics, University of Science and Technology of China, Hefei, Anhui 230027, China

[b] National Microgravity Laboratory, Institute of Mechanics, Chinese Academy of Sciences, Beijing 100080, China

ARTICLE INFO

Available online 10 August 2011

Keywords:
Interferometry
Temporal phase evaluation
Mass transfer
Crystal growth rate

ABSTRACT

The mass transfer process and the crystal growth rate have been proved to be very important in the study of crystal growth kinetics, which influence the crystal quality and morphological stability. In this paper, a new method based on temporal phase evaluation was presented to characterize the mass transfer process in situ and determine the crystal growth rate. The crystallization process of NaCl crystal growth by evaporation was monitored in situ by a Mach–Zehnder interferometer, and the absolute concentration evolution, the evaporation rate and the real-time supersaturation of solution were obtained using temporal phase analysis, which acted as a novel technique to extract phase variation along time axis recently. Based on the evaporation rate and the absolution concentration, a new method to calculate mass transfer flux during the crystal growth without the knowledge of the mass transfer coefficient was proposed, and then the crystal growth rate could also be retrieved under the hypothesis of cubic crystals. The results show that the crystal growth rate increases with the supersaturation linearly. It is in agreement with the diffusion theories, which presume that matter is deposited continuously on a crystal face at a rate proportional to the difference in concentration between the points of deposition and the bulk of solution. The method is applicable to the research of crystallization process based on evaporation or vapor diffusion of which the precise conditions of nucleation and supersaturation are usually unknown because of the complexity of the evaporation rate and crystal growth rate.

1. Introduction

With the development of new techniques such as microelectronics, laser, optical communications and biomedicine, large crystals with a high degree of perfection are required in many fields. In practice, it will meet some problems such as cracks, twins or excessive nucleation, which obstruct to obtain big and good quality crystals. The quality of crystals is influenced by many factors, i.e. concentration, supersaturation, mass transfer process and crystal growth rate, which play important parts in optimizing and investigating crystallization mechanism [1]. To facilitate growth parameters measurements and develop crystal growth theories, various researches have been carried out in the past few decades.

In experimental methods, optical interferometry, which is suitable for the quantitative and non-invasion measurement of transparent sample, has been proved to be an effective phase retrieval technique in real-time observation of concentration distribution [2], diffusion fields [3] and convection [4] around a crystal. According to the concentration boundary [5] and the diffusion theories, the mass transfer process and the growth rate of lysozyme crystals could also be investigated with four-step phase-shifting algorithm [6]. Atomic force microscopy, which perform a high resolution, is another wildly used technique to examine surface topography, measure crystal growth rates and investigate growth mechanisms [7]. Compared with optical interferometry, it is superior in resolution but much more time-consuming, and the contact mode of AFM will result in sample damage. In the theoretical research, the following four crystal growth theories are usually studied. Surface energy theories are based on the postulation that the final shape of a crystal adheres to the principle: the total free energy of a crystal is a minimum for a giving volume [8]. Volmer proposed and developed adsorption layer theories to reveal crystal growth mechanism based on the existence of an adsorbed layer of solute atoms or molecules on a crystal face [1]. Subsequently, Burton, Cabrera and Frank suggested a kinetic theory of growth to explain why crystal can grow even at low supersaturation values [9]. The diffusion theories [10],

* Corresponding author. Tel.: +86 551 3601248; fax: +86 551 3606459.
E-mail address: miaohong@ustc.edu.cn (H. Miao).

0143-8166/$ - see front matter © 2011 Elsevier Ltd. All rights reserved.
doi:10.1016/j.optlaseng.2011.07.013

which presume that matter is deposited continuously on a crystal face at a rate proportional to the difference in concentration between the point of deposition and the bulk of solution, are simple and widely used in industry practice to study mass transport properties and crystal growth kinetics.

Although many observation techniques and theoretical analysis have already been preformed, more studies are still needed to explore crystal growth process, especially crystal growth from solution, which is a complex non-equilibrium process. In this work, a real-time measurement system with a Mach–Zehnder interferometer and temporal phase analysis was developed to obtain the concentration and supersaturation of solution in crystal growth. Based on the velocity of water evaporation and the absolution concentration, a method was proposed to analyze mass transfer process and crystal growth rate, and its applicable conditions and reliability were also discussed.

2. Experimental setup and parameters

Crystallization experiment was conducted by evaporation method, so the absolute concentration and supersaturation is changing with time. 24.7%(w/w) NaCl solution was prepared with deionized water at 291 K. The unsaturated NaCl solution gradually reaches saturation and then nucleates spontaneously by evaporation at a constant temperature. To monitor the entire crystallization process and measure the crystal growth kinetics, a conventional Mach–Zehnder interferometer was adopted. The schematic diagram of the apparatus is shown in Fig. 1. A He–Ne laser beam (λ=632.8 nm), passing through a spatial filter and a collimation lens to form a parallel light beam with about 7 mm diameter, was split into two beams by a beamsplitter (BS1). The one through the growth cell served as the object beam and the other one served as the reference beam. They met at the other beamsplitter (BS2) and formed interferograms that were magnified by a long working-distance microscope objective (MO) and recorded by a CCD camera with pixel size of $6.7 \times 6.7\ \mu m^2$. A total of 780 frames interferogram were captured in 13 h.

3. Principle and theory

3.1. The principle of the concentration measurement

The refractive index of solution varies linearly with the concentration of solute, so the interferometer, which records the change in the refractive index, can be used to determine changes in the concentration profile. The phase-shifting method [2,4,6] and fringe-counting method [11,12] are usually used to retrieve concentration in crystal growth process. The phase-shifting method can only obtain the relative concentration distribution rather than the absolute concentration and real-time supersaturation. The supersaturation is the driving force of crystal growth, which has

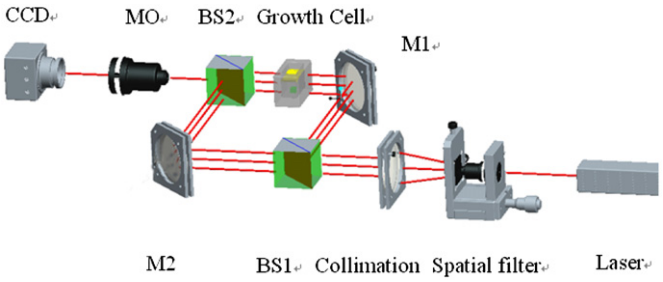

Fig. 1. Optical observation and measurement system based on a Mach–Zehnder interferometer.

a great influence on crystal growth rate and quality. The relationship between supersaturation and crystal growth rate can reveal the crystal growth mechanics. Fringe-counting method fails to give the full-field concentration distribution and its precision is low. In this work, the absolute concentration is measured by temporal phase analysis, which determines the instantaneous refractive index of solution by analyzing the intensity variation of interference speckle along the time axis pixel by pixel. The detailed principle of the method and several applications in speckle interferometry and vibration measurement can be found in Refs. [13–16]. Fourier transform [17] is usually applied to extract the phase in temporal domain. In recent years, wavelet analysis [18] and windowed Fourier transform [19] have also been introduced in temporal phase extraction to limit the influence of various noise sources and improve the result in displacement measurement. However, for temporal intensity variation signals, both wavelet analysis and windowed Fourier analysis may generate large errors if the parameters are not properly selected. Windowed Fourier analysis suffers due to its fixed window size, while wavelet analysis sometimes is also not a good choice because of its poor performance at low-frequency part in thephaseextraction. The best temporal processing algorithm for intensity variation signal is the combination of Fourier and windowed Fourier analysis [13]. In this experiment, the absolute concentration distribution was retrieved based on the combination of Fourier transform and windowed Fourier transform.

The sequence of interferograms recorded by a CCD camera can be expressed, mathematically, as

$$I(x,y,t) = a(x,y) + b(x,y)\cos[\phi(x,y,t)] \tag{1}$$

where $a(x,y)$ and $b(x,y)$ are background intensity and modulation factor of the temporal interference patterns, respectively, and $\phi(x,y,t)$ is time-dependent phase function related to the concentration variation of solution. The Fourier transform of Eq. (1) with respect to the time variable t can be written as

$$F(x,y,\xi) = \int I(x,y,t)\exp(-j\xi t)dt = DC(x,y,\xi) + C(x,y,\xi) + C^*(x,y,\xi). \tag{2}$$

The second term on the right-hand side can be isolated via a suitable bandpass filtering and then an inverse Fourier transform can be applied (Eq. (3)) to yield an exponential signal $I_F(x,y,t)$ from which the phase can be calculated by Eq. (4).

$$I_F(x,y,t) = \int C(x,y,\xi)\exp(j\xi t)d\xi, \tag{3}$$

$$\varphi(x,y,t) = \arctan\frac{\mathrm{Im}[I_F(x,y,t)]}{\mathrm{Re}[I_F(x,y,t)]}. \tag{4}$$

The accuracy depends on the selection of a proper window for bandpass filtering. It means that noise whose frequency is within the filtering windows cannot be removed by FT analysis. To improve the resluts, the phase variation $\varphi(t)$ is converted to an exponential signal $f(t) = \exp[i\varphi(t)]$. Windowed Fourier transform method is then applied. On the assumption that the phase is linear in a small window, mathematically, $\varphi(t) = \varphi(u) + \varphi'(u)(t-u)$, the WFT can be expressed as

$$STFT(u,\xi) = \sqrt{2\pi}\sigma\exp\left\{\frac{-\sigma^2[\xi-\varphi'(u)]^2}{2}\right\}\exp(j[\varphi(u)-\xi u]), \tag{5}$$

where σ controls the size of Gaussian window, u and ξ represent the time and frequency, respectively. The phase $\varphi(t)$ and phase derivative $\varphi'(t)$, corresponding to the absolute concentration and the

change rate of concentration, respectively, can be calculated by

$$\begin{cases} \varphi(t) = angle[STFT(u,\xi)]_{\xi=\varphi'(u)} \\ \varphi'(u) = \max\{abs[STFT(u,\xi)]\}_{\xi} \end{cases} \quad (6)$$

3.2. The proposed method to characterize mass transfer process and determine crystal growth rate

Crystal growth is a process related to heat and mass transfer that dominates the morphological instability near the growing interface and the quality of crystal. The most commonly used methods to calculate mass transfer flux and crystal growth rate are listed as follows. According to the difference between the initial and final crystal size, the average growth rate during the total growth time can be retrieved. In reference to the diffusion theory of crystal growth, the mass diffusion and crystal growth rate can be calculated from the concentration distribution of the solid–liquid interface around the crystal [6]. The crystal growth mechanisms and the crystal growth rate can also be in situ observed by AFM [7].

For crystallization experiments by evaporation, the change in concentration before nucleation is caused by water evaporation, while the change after nucleation is induced by both water evaporation and solute adsorption on crystal. Based on the evaporation rate and the absolution concentration obtained by temporal phase analysis, a new method was proposed to investigate the mass transfer flux and crystal growth rate in the entire crystallization process. It is especially suitable for crystallization by evaporation or vapor diffusion method in protein crystallization [20].

To simplify the theoretical analysis process, we make a hypothesis of constant evaporation rate. As it is known, under a constant temperature, the velocity of water diffusion depends on the difference between the vapor pressure near the surface of sample solution and the vapor pressure of water in the air. For ideal solution, it obeys Raoult's Law that the vapor pressure of the solute-containing solution is equal to the vapor pressure of the pure solvent times the mole fraction of the solvent. For electrolyte, Raoult's Law must be corrected by multiplying by a factor. The reasonability of the hypothesis can be validated by the linear relationship between concentration curve and time before nucleation in Section 4.1.

The formula derivation process of the method calculating mass transfer flux and crystal growth rate can be expressed as follows.

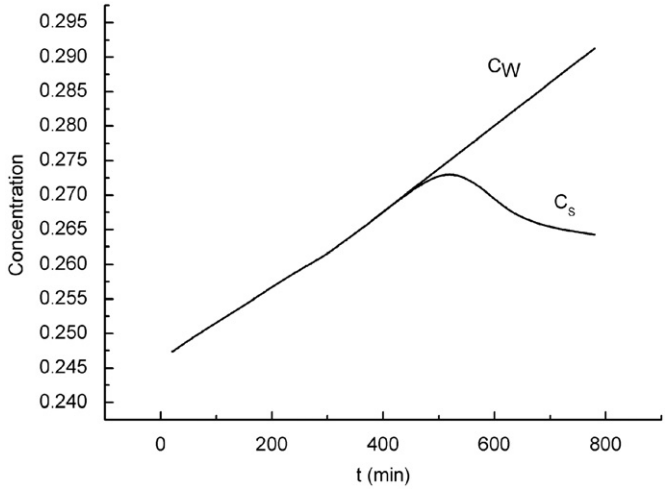

Fig. 2. Schematic diagram of the new method proposed to calculate mass transfer flux and crystal growth rate. C_w, the concentration caused by water evaporation; C_s, the absolute concentration evolution.

As shown in Fig. 2, curve (C_w) represents concentration variance caused by water evaporation in the entire process of crystal growth, and curve (C_s) denotes the absolute concentration evolution, i.e. the concentration curve obtained by temporal phase analysis, which is induced by both water evaporation and solute molecules adsorption on crystals. Because the variance in concentration before nucleation is only caused by water evaporation, the mass of solution when nucleation can be calculated by

$$M_1 = \frac{C_0 \times M_0}{C_1}, \quad (7)$$

where C_0 and M_0 are the initial concentration and mass of solution, respectively. C_1 and M_1 denote the concentration and mass of solution when nucleation, respectively.

Then, the total mass transfer $M(t)$ after nucleation can be calculated by Eq. (8):

$$\frac{[C_1 \times M_1 - M(t)]}{[x(t) - M(t)]} = C_s(t) \quad (8)$$

$$x(t) = \frac{C_1 \times M_1}{C_w(t)} \quad (9)$$

where $x(t)$ is the residual mass of solution without considering the decrease in solute caused by crystal growth.

Then the mass transfer can be expressed as

$$M(t) = \frac{[C_1 \times M_1 - C_s(t) \times C_1 \times M_1 / C_w(t)]}{[(1 - C_s(t)]}. \quad (10)$$

The rate of mass transfer $M'(t)$ as a function of time t can be written as

$$M'(t) = \frac{d(M(t))}{dt} \quad (11)$$

On the assumption that the crystal is cubic, the growth rate of the crystal can be expressed as follows:

$$R = \frac{d}{dt}\left\{\left(\frac{M(t)}{\rho}\right)^{1/3}\right\} \quad (12)$$

where ρ is the density of the crystal.

4. Results and discussion

4.1. The crystallization process, the absolute concentration and the supersaturation evolution of the solution

As soon as the solution was injected into growth cell, the evaporation began because the vapor pressure was unsaturated. The typical sequence of the crystallization process by evaporation under a constant temperature is shown in Fig. 3. The changes in fringe spacing denote the variations of the concentration gradient, and the moving direction of fringes depends upon an increase or decrease in absolute concentration of solution. The upper part of image without fringe in Fig. 3(c) and (d) is caused by the fall of the liquid level, while the area surrounded with fringes represents crystal. After analysis of the sequence of interferograms, crystallization process can be divided into four stages qualitatively according to the changes in fringes: (1) the straight and uniform fringes moved up with a constant speed and the NaCl solution gradually reached saturation. (2) Crystals appeared in the upper part of solution at t=386 min as shown in Fig. 3(b). Fringes became dense and their moving speed slowed down. (3) Interference fringes moved in the opposite direction with the growth of crystals. The reason is that the speed of solute adsorption was greater than that of the concentration variation induced by evaporation. Meanwhile, the fringes around the crystal contorted as shown in Fig. 3(c), which meant concentration gradient

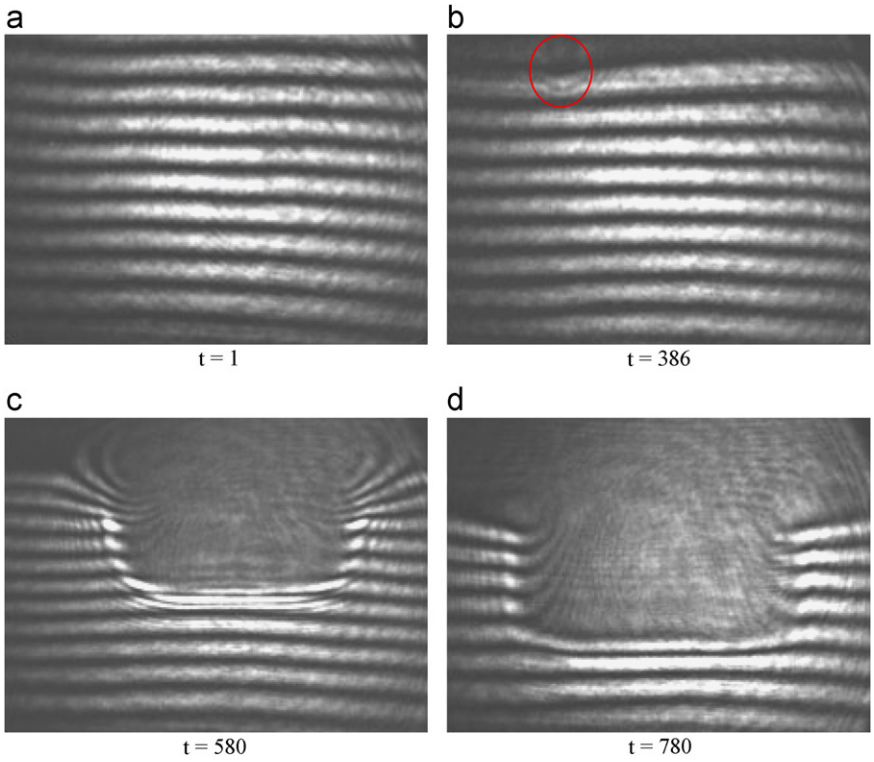

Fig. 3. Crystallization process and sequence of interferograms of NaCl crystal growth by evaporation. The upper part of graph without fringes in (c) and (d) is caused by the fall of the liquid level, while the area surrounded with fringes presents crystal. (a) The initial interferogram with straight and uniform fringes. (b) The highlighted ellipse is the area nuclear appeared. (c) Fringes became dense and distorted near the crystal. (d) Fringes became sparse gradually tended to static with the growth of crystal.

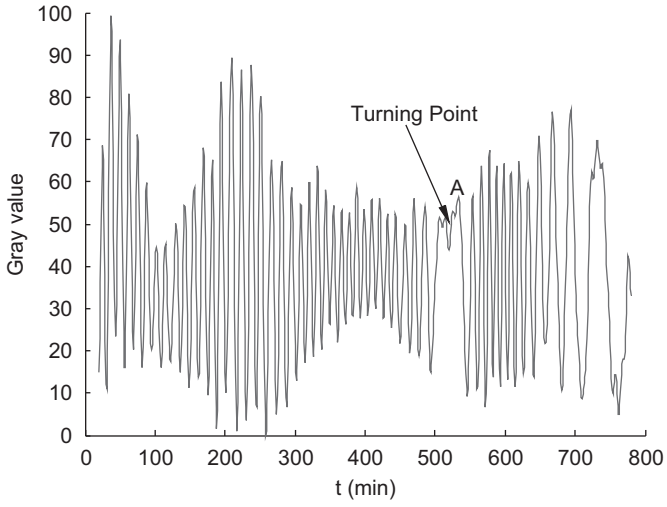

Fig. 4. Typical intensity evolution curve of solution in the entire crystallization process by evaporation.

changed for the reason that the mass transfer flux increased with the development of surface area of crystals. (4) Fringes became sparse again and gradually tended to be static.

Fig. 4 shows the temporal intensity evolution of solution in the entire crystallization experiment by evaporation. The sinusoidal period of the intensity variance signal maintains unchanged before nucleation. The moving speed of fringes turns to the opposite direction at $t=522$ min corresponding to the turning point A as shown in Fig. 4. With crystal growth, the sinusoidal period of the temporal signal gradually becomes bigger. After temporal phase analysis on the intensity evolution curve, the absolute concentration (c) of far-field solution can be obtained as shown in Fig. 5(a). Supersaturation is the driving force of crystal growth, which has a great influence on crystal growth rate and quality. The absolute supersaturation ($\Delta c=c-c^*$, where c^* is solubility of NaCl) after nucleation can be easily retrieved from the absolute concentration curve, which is shown in Fig. 5 (b). It is found that the change in concentration of solution is in agreement with the four stages, which can be observed in the sequence of interference fringes.

4.2. The mass transfer process and crystal growth rate

As shown in Fig. 5(a), the concentration increases linearly with the time before nucleation. It is confirmed that the hypothesis in the proposed method to investigate mass transfer process is reasonable. Once the concentration evolution through the entire crystallization process is measured by the temporal phase analysis, the mass transfer flux (g) and the mass transfer rate (cm^3/min) changing with time can be obtained by the proposed method, which are shown in Fig. 6 and in Fig. 7, respectively. The results showed that the mass transfer flux and the mass transfer rate increased very slowly with time at first because both the surface of crystal and supersaturation are small. As the supersaturation and the crystal growth area increased, the curves of the mass transfer flux and the mass transfer rate rose rapidly. When $t=590$ min, the mass transfer rate reach the maximum, and then descended and tended to equilibrium at last owing to a decrease in supersaturation. It is worth noting that the maximum mass transfer rate ($t=590$ min) does not correspond to the highest supersaturation ($t=519$ min), which indicates that the mass transfer rate depends on both supersaturation and the growth area of crystal.

The density of NaCl crystal is 2.165 g/cm^3. The crystal growth rate as a function of time (m/s) can be calculated by Eq. (12) and plotted in Fig. 8. The result shows that the trend of crystal

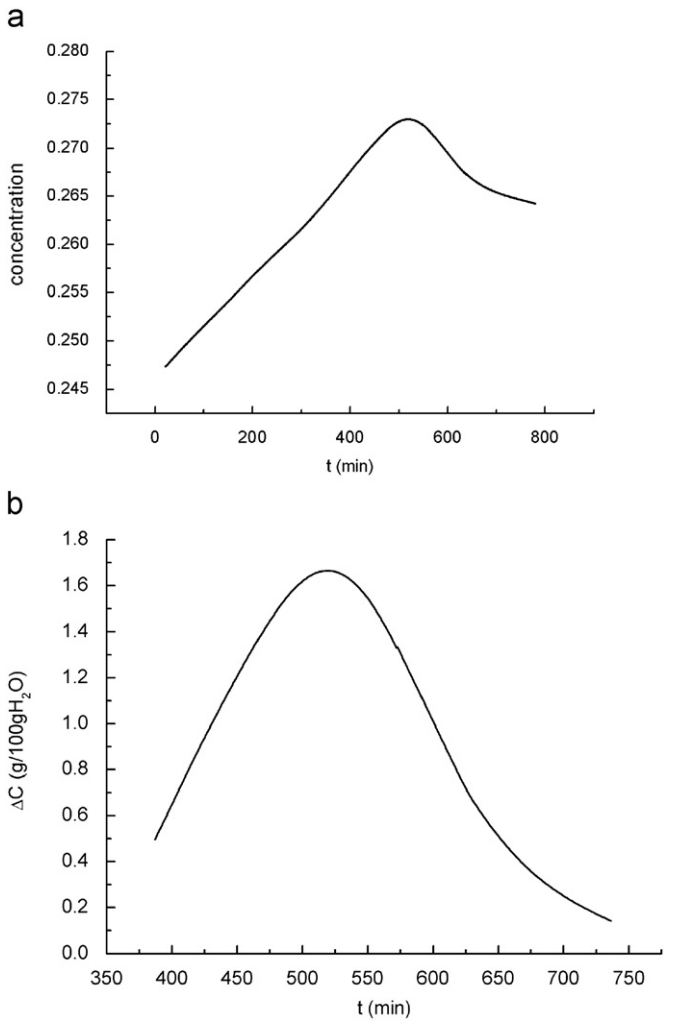

Fig. 5. (a) Absolute concentration evolution of NaCl solution in crystallization experiment at 291 K. (b) Absolute supersaturation after nucleation (t=386 min).

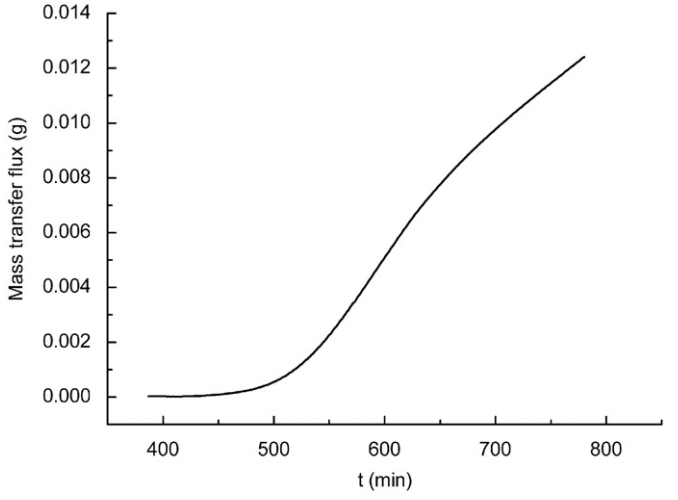

Fig. 6. Mass transfer flux (g) after nucleation vs. time (min).

growth rate except the fluctuated segment before $t<460$ min is analogous to the supersaturation shown in Fig. 5(b). The crystal growth rate reaches the highest point (t=516 min) when the supersaturation reaches the maximum at the time of t=519 min,

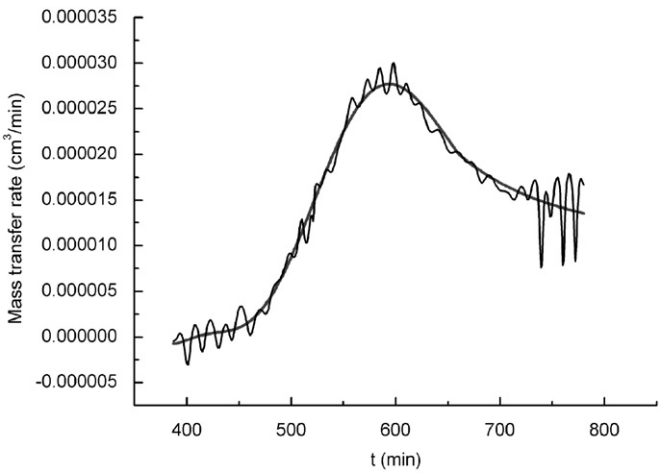

Fig. 7. Mass transfer rate (cm^3/min) after nucleation vs. time (min).

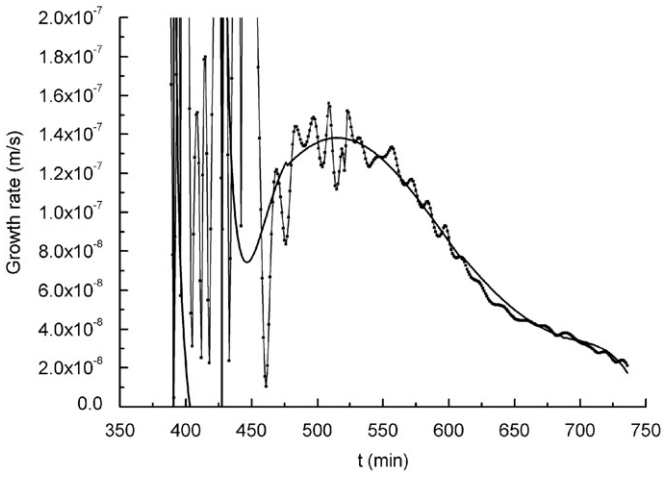

Fig. 8. Crystal growth rate (m/s) vs. time (min). Dotted line, initial data calculated with the proposed method; solid line, filtered data.

and then declines continuously to equilibrium. To illuminate the mechanism of NaCl crystal growth, the relationship between crystal growth rate and absolute supersaturation was also investigated as shown in Fig. 9. The result indicates that the crystal growth rate increases linearly with the increasing supersaturation.

We choose a point t=624 min when the supersaturation expressed by $S=c/c^*$ is 1.02, where c and c^* are the concentration of solution (g/100 g H_2O) and solubility (g/100 g H_2O), respectively. The rate of crystal growth measured in our work is 3.15×10^{-8} m/s. Mullin reported that the mean overall crystal growth rate of NaCl is 6.5×10^{-8} m/s under the conditions of T=323 K and S=1.003 [1]. It is the same order of magnitude with our results.

To verify the correctness of the proposed method, we also compared the results with "diffusion theories". According to the diffusion theories [10], there are two stages occurring under the influence of different concentration driving forces during crystal growth. They can be represented by the equations:

$$\frac{dm}{dt}=k_dA(c-c_i)\ \text{(Diffusion process)} \tag{13}$$

$$\frac{dm}{dt}=k_rA(c_i-c^*)\ \text{(Reaction process)} \tag{14}$$

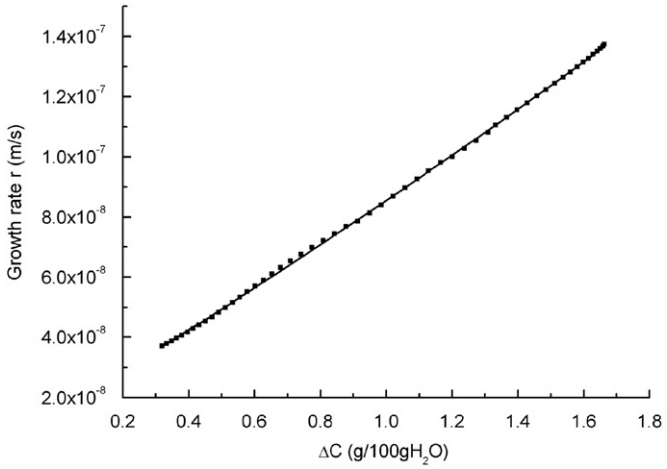

Fig. 9. Overall crystal growth rate (m/s) vs. supersaturation.

where k_d is the mass transfer coefficient, k_r is rate constant for the surface reaction process and c_i is solution concentration in the solution at the crystal–solution interface. Eq. (13) represents 'diffusion process', whereby solute molecules are transported from the bulk of fluid phase to the solid surface, followed by a first-order 'reaction' when the solute molecules arrange themselves into the crystal lattice.

In fact, a general equation for crystallization based on overall driving force is usually applied in the practical study of mass transfer process [6,21], which can be written as

$$\frac{dm}{dt} = k_G A(c - c^*)^g \tag{15}$$

where k_G is an overall crystal growth coefficient. The exponent g is usually referred to as the 'order' of overall crystal growth process. The rate equations, therefore, may be written as

$$R_G = k_G(c - c^*)^g = k_G(\Delta c)^g \tag{16}$$

According to the Burton–Cabrera–Frank (BFC) relationship [9], when the supersaturation (Δc) is higher, crystal growth rate is linear with supersaturation and 'Diffusion process' dominated the crystal growth. When the supersaturation is lower, crystal growth rate is proportional to the square of supersaturation. Compared with ''diffusion theories'', the linear relationship between the resulting crystal growth rate and the supersaturation is in agreement with the diffusion theories at higher supersaturation. Since the concentration used in our method is the bulk concentration of solution rather than the concentration at the crystal–solution interface, the method may be more suitable for 'Diffusion process' than 'Reaction process'. The fluctuation before $t < 460$ min in Fig. 8 can be interpreted as that the method is derived by diffusion process, but the crystal growth in early period is the dominated by 'reaction process' when both the supersaturation and the crystal surface are small.

5. Conclusion

Measurement of crystallization kinetics parameters, i.e. absolute concentration, supersaturation, mass transfer process and crystal growth rate, has been proved to be very important in illuminating crystallization mechanism and optimizing crystal quality. In present paper, an observation and measurement system, based on a Mach–Zehnder interferometer and temporal phase analysis, has been developed to retrieve the absolute concentration evolution and real-time supersaturation through the entire crystallization process from spontaneous nucleation to crystal growth into visible size. The other focus of the work is on the study of mass transfer process and crystal growth rate, which have been calculated by a new proposed method based on the system. Compared with diffusion theory, the mass transfer flux and mass transfer rate can be calculated at any instant after nucleation without the knowledge of mass transfer coefficient. On the hypothesis of cubic crystal, the crystal growth rate can also be obtained. The results, which are verified to be in agreement with diffusion theory and the previous literature, show that the crystal growth rate obtained from the method increases with supersaturation linearly. Although it has a limitation that it is only suitable for 'diffusion process' of crystal growth because the bulk concentration of solution rather than the concentration at the crystal–solution interface is employed in the method, it is obvious that the system and the new method for characterizing the mass transfer process and determining the crystal growth rate will make a contribution on the research of crystal growth process. The system and the method are especially suitable to investigate the crystallization process by evaporation or vapor diffusion (protein crystallization), which is usually a complex and non-equilibrium process because it is influenced by both water evaporation and crystal growth.

Acknowledgment

The authors would like to acknowledge the financial supports provided by the National Science Foundation of China (NSFC) under contract numbers 11072235 and 10732080, and the National Basic Research Program of China under contract number 2007CB936803.

References

[1] Mullin JW. Crystallization. 3rd ed. London: Butterworth Heinemann; 2000.
[2] Onuma K, Tsukamoto K, Nakadate S. Application of real-time phase-shift interferometer to the measurement of concentration field. J Cryst Growth 1993;129:706–18.
[3] Srivastava A, Tsukamoto K, Yokoyama E, Murayama K, Fukuyama M. Fourier analysis based phase shift interferometric tomography for three-dimensional reconstruction of concentration field around a growing crystal. J Cryst Growth 2010;312:2254–62.
[4] Duan L, Shu JZ. The convection during NaClO3 crystal growth observed by the phase shift interferometer. J Cryst Growth 2001;223:181–8.
[5] Chrysikopoulos CV, Hsuan PY, Fyrillas MM, Lee KY. Mass transfer coefficient and concentration boundary layer thickness for a dissolving NAPL pool in porous media. J Hazard Mater 2003;B97:245–55.
[6] Duan L, Kang Q, Hu WR, Li GP, Wang DC. The mass transfer process and the growth rate of protein crystals. Biophys Chem 2002;97:189–201.
[7] Malkin AJ. Investigation of virus crystal growth mechanisms by in situ atomic force microscopy. Phys Rev Lett 1995;75:2778–81.
[8] Gibbs JW. Thermodynamics.Collected Works, vol. I. New Haven: Yale University Press; 1948.
[9] Lasaga AC. Kinematic theory in earth science. New Jersey: Princeton University Press; 1998, p. 581–704.
[10] Nývlt J, Söhnel o, Matachová M, Broul M. The kinetics of industrial crystallization. Elsevier; 1985.
[11] Garcia-Ruíz JM, Novella ML, Otálora F. Real time evolution of concentration distribution around tetragonal lysozyme crystal: case study in gel and free solution. J Cryst Growth 1999;196:703–10.
[12] Snell EH, Helliwell JR, Boggon TJ, Lautenschlager P, Potthast L. Lysozyme crystal growth kinetics monitored using a Mach–Zehnder interferometer. Acta Crystallogr 1996;D52:529–33.
[13] Fu Y, Groves RM, Pedrini G, Osten W. Kinematic and deformation parameter measurement by spatiotemporal analysis of an interferogram sequence. Appl Opt 2007;46:8645–55.
[14] Fu Y, Pedrini G, Osten W. Vibration measurement by temporal Fourier analyses of a digital hologram sequence. Appl Opt 2007;46:5719–27.
[15] Fu Y, Shi H, Miao H. Vibration measurement of a miniature component by high-speed image-plane digital holographic microscopy. Appl Opt 2009;48:1990–7.

[16] Kaufmann GH, Galizzi GE. Phase measurement in temporal speckle pattern interferometry: comparison between the phase-shifting and the Fourier transform methods. Appl Opt 2002;41:7254–63.
[17] Joenathan C, Franze B, Haible P, Tiziani HJ. Speckle interferometry with temporal phase evaluation for measuring large-object deformation. Appl Opt 1998;37:2608–14.
[18] Fu Y, Tay CJ, Quan C, Miao H. Wavelet analysis of speckle patterns with a temporal carrier. Appl Opt 2005;44:959–65.
[19] Kemao Q. Two-dimensional windowed Fourier transform for fringe pattern analysis: principles, applications and implementations. Opt Laser Eng 2007;45: 304–17.
[20] McPherson A. Introduction to protein crystallization. Methods 2004;34: 254–65.
[21] Zhou Y, Kovenklioglu S. Growth and nucleation kinetics in batch crystallization of triclosan. Chem Eng Commun 2004;191:749–66.